Available online at www.sciencedirect.com
SCIENCE DIRECT
Journal of Sound and Vibration 293 (2006) 807–818
JOURNAL OF SOUND AND VIBRATION
www.elsevier.com/locate/jsvi

Simplified contact filters in wheel/rail noise prediction

R.A.J. Ford[a,*], D.J. Thompson[b]

[a]School of Mechanical and Manufacturing Engineering, The University of New South Wales, UNSW Sydney 2052, Australia
[b]Institute of Sound and Vibration Research, University of Southampton, Highfield, Southampton SO17 1BJ, UK

Accepted 26 August 2005
Available online 15 February 2006

Abstract

When predicting rolling noise due to wheel and rail roughness a ''contact filter'' is generally applied to account for the effect of the finite size of the wheel/rail contact. For time-domain analysis these calculations must be fast enough to get results in a reasonable time. Remington and Webb have devised a versatile three-dimensional 'distributed point reacting spring' (DPRS) contact model that is relatively quick, but if only one line of data is available along the contact it is unnecessarily complex, so a simpler two-dimensional version has been developed here. When this new model was checked against a Boussinesq analysis of the contact, the results in one-third octave bands were found to agree to within 3 dB. These results further suggest that the two-dimensional DPRS model might have an unexpectedly wide range of applicability, including large amplitude sinusoidal roughness and discrete features such as a rail joint. When implemented at each step in a time-domain wheel/rail interaction analysis, this model gave similar results to quasi-static roughness filtering with a constant load for moderate roughness, but dynamic effects became significant when the roughness amplitudes were large, particularly with dipped rail joints.

1. Introduction

When predicting rolling noise due to wheel and rail roughness a ''contact filter'' is generally applied to account for the finite size of the wheel/rail contact. Because the contact exists over a finite area, roughnesses with wavelengths that are short compared with the length of this contact patch are attenuated in their excitation of the system.

Remington produced an analytical model for this contact filter [1]. Subsequently, Remington and Webb produced an alternative approach [2] based on a 'distributed point reacting springs' (DPRS) numerical model, or 'mattress model', which represents the contact by a set of independent nonlinear springs. When roughness data measured on many parallel lines is processed by this model the result is the ''blocked force'' as a function of longitudinal position. Dividing by the nominal contact stiffness yields an equivalent filtered roughness [3].

Where time-stepping calculations of the response of the wheel/rail system are to be carried out, this filter is required to operate in the time domain. Such situations include the response to large amplitude roughness [4] and discrete features on the wheel or rail, such as wheel flats [5] or rail joints [6] where large amplitudes

*Corresponding author. Tel.: +61 2 9385 4091; fax: +61 2 9663 1222.
E-mail address: r.ford@unsw.edu.au (R.A.J. Ford).

0022-460X/$ - see front matter © 2006 Elsevier Ltd. All rights reserved.
doi:10.1016/j.jsv.2005.08.049

introduce nonlinearities and even loss of contact. Often, measurements of roughness data are available only on a single line that is taken as typical of the running band. While the three-dimensional (3D) DPRS model may be applied in such situations, it is more complex than necessary and hence slower too.

For these reasons, a two-dimensional (2D) 'mattress' model is investigated here. The Hertzian contact is again replaced by a set of independent springs, but these are now located along a single line. Its effectiveness has been checked using a Boussinesq analysis, similar to that used by Remington and Webb [2] to assess their DPRS model. Results are compared with other models of the contact filter. Finally, the mattress model is incorporated into a time-domain model of wheel/rail interaction.

2. Two-dimensional mattress model

2.1. Hertzian model

Consider the Hertzian contact geometry in Fig. 1(a). Local deformation of both the wheel and rail occurs, although for clarity the figure shows the deformation as present on the wheel alone. The contact patch length is $2a$ and the 'distance of approach' of the wheel to the rail is δ.

Consider, for simplicity, the case in which the transverse curvature of the rail (assumed straight) is the same as the radius of curvature of the wheel in the rolling direction, R, and the wheel is conical, so the contact patch is circular. From Hertzian contact theory [7]

$$\delta = \frac{a^2}{R}. \tag{1}$$

This is exactly true for a circular contact patch and approximately true for an elliptical contact patch, where R is replaced by an equivalent radius R_e. The Hertzian pressure distribution is [7]

$$p(r) = p_0\sqrt{1-\left(\frac{r}{a}\right)^2}, \quad r \leqslant a, \tag{2}$$

where r is the distance from the centre of the contact patch and p_0 is the maximum pressure, given by $P = \frac{2}{3}p_0\pi a^2$ [7], where P is the contact force. To express contact force in terms of static deflection, the Hertzian expression for static deflection [7] may be rearranged to give

$$P = \frac{2E^*R^{1/2}}{3}\delta^{3/2}, \tag{3}$$

where $E^* = E/(1-\nu^2)$ is the plane strain Young's modulus (both materials assumed equal) and R is the radius of curvature of wheel and railhead (NB the notation for E^* differs from Ref. [7]; see also Ref. [8]).

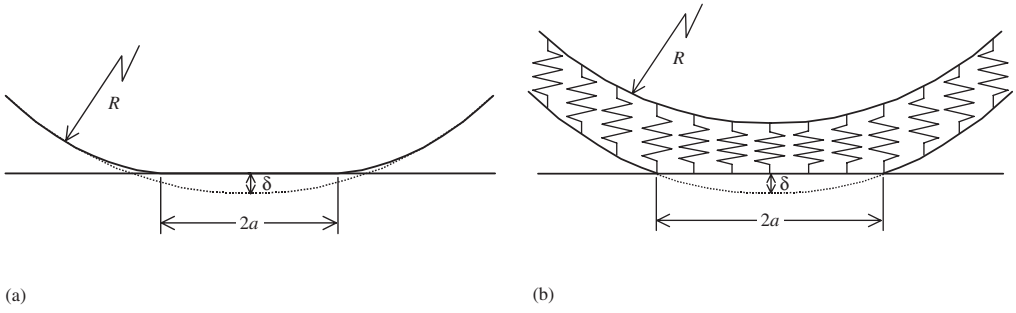

Fig. 1. Contact between wheel and rail: (a) Hertzian contact; (b) 'mattress' model. For simplicity only the wheel is shown to deflect.

2.2. Two-dimensional discrete spring model

As an approximation for the contact, a 'mattress' model of independent springs is shown in Fig. 1(b). Here, the force at a given point causes deformation only at that point. Let the stiffness of these springs be k per unit length (the contact is assumed to have a constant width rather than being elliptical). The equivalent radius of curvature of the wheel to be used in the mattress model (to be determined) is R_m. The wheel surface is defined by

$$(R_m - y)^2 + x^2 = R_m^2 \Rightarrow y \approx \frac{x^2}{2R_m}. \tag{4}$$

The semi-length of the contact is then given by substituting $x = a$ and $y = \delta$:

$$\delta \approx \frac{a^2}{2R_m} \quad \text{or} \quad a \approx \sqrt{2R_m\delta}. \tag{5}$$

Note that this differs from the exact expression in Eq. (1) by a factor of 2 (also see Ref. [7]). The total contact force is given by

$$P = \int_{-a}^{a} f(x)\,\mathrm{d}x, \quad \text{where } f(x) = \begin{cases} k(\delta - y(x)) & \text{if } \delta - y(x) > 0, \\ 0 & \text{if } \delta - y(x) \leqslant 0. \end{cases} \tag{6}$$

Substituting for y and δ from Eqs. (4) and (5), this yields

$$P = \int_{-a}^{a} k\left(\frac{a^2}{2R_m} - \frac{x^2}{2R_m}\right)\mathrm{d}x = \frac{k}{2R_m}\int_{-a}^{a}(a^2 - x^2)\,\mathrm{d}x = \frac{2ka^3}{3R_m}, \tag{7}$$

in which the pressure distribution is parabolic, rather than circular as given by Eq. (2). Substituting for a from Eq. (5) in Eq. (7) gives

$$P = \frac{2k}{3R_m}(2R_m\delta)^{3/2} = \frac{4\sqrt{2}k}{3}R_m^{1/2}\delta^{3/2}. \tag{8}$$

The actual relationship between contact force and static deflection according to the Hertzian model is given by Eq. (3), and this can be replicated in Eq. (8) by choosing

$$k = \frac{E^* R^{1/2}}{2\sqrt{2}R_m^{1/2}}, \tag{9}$$

which shows that the overall nonlinear 3D contact stiffness behaviour may be reproduced correctly using a linear 2D mattress model.

2.3. Adjustments to model

For noise predictions it is important that the contact patch has the correct length as this affects the wavelengths filtered. Ideally, it is desirable to have correct values simultaneously for contact length, total contact load, deflection, and wheel and rail geometry (radii of curvature). Unfortunately, as with the 3D DPRS model [2], this is not possible. For example, comparing Eqs. (1) and (5), it is seen that the mattress model does not give a correct contact patch length if the static deflection is correct. The best compromise is to adjust the wheel radius such that the other three quantities are correct and consistent. For the 2D mattress model the adjusted wheel radius is

$$R_m = \tfrac{1}{2}R, \tag{10}$$

where R is the wheel and railhead radius of curvature for the original contact (assumed equal). Eqs. (1) and (5) then become consistent. Substituting this into Eq. (9), k reduces to

$$k = \tfrac{1}{2}E^*. \tag{11}$$

For non-circular contacts, the relations are more complicated but it is important to ensure that the contact patch semi-length a and the approach δ are maintained.

2.4. Roughness processing

If the roughness profile (positive for an asperity) is given by $r(x)$, the total contact force when the wheel is centred at x is given by a modified form of Eq. (6)

$$P(x) = \int_{-a'}^{a'} f(x')\,\mathrm{d}x',$$

where

$$f(x') = \begin{cases} k(\delta - y(x') + r(x+x')) & \text{if } \delta - y(x') + r(x+x') > 0, \\ 0 & \text{if } \delta - y(x') + r(x+x') \leqslant 0, \end{cases} \tag{12}$$

where the integration is performed over $-a' < x' < a'$, this range being extended to sufficiently large a' to cover all potential points of contact (it may be necessary to check after the calculations that this condition has been met).

In order to process a set of roughness data, for each longitudinal position x the roughness in a region around x is chosen, $r(x+x')$ for $-a' < x' < a'$. This is combined with the circular profile of the wheel, $y(x')$, see Eq. (4), and a value of δ is sought such that the total force P is equal to the nominal wheel load. The difference between this and the nominal value of δ (i.e. in the absence of roughness) is stored as the 'equivalent roughness' at location x. Alternatively, the value δ could be imposed and the blocked force P determined. By comparing the spectra of the initial roughness and the equivalent roughness, a filter effect can be derived.

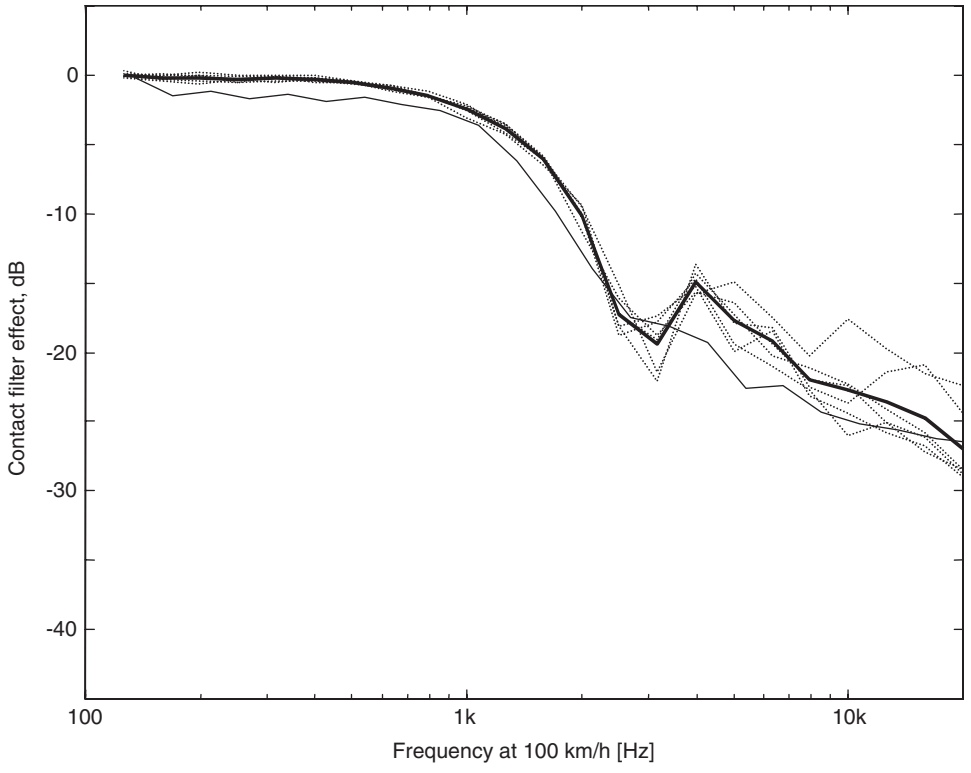

Fig. 2. Contact filter effect for $R = 0.46\,\mathrm{m}$, $P = 50\,\mathrm{kN}$. · · · · · · results from six sets of roughness data using 2D model, — average result for 2D model, ▬ average result from 3D DPRS model.

2.5. Results of two-dimensional discrete spring model

In Ref. [3] six sets of wheel roughness data were used to derive the filter effect of the DPRS model. These same data have been used here to derive the filter effect of the new 2D mattress model. Although Ref. [3] used several parallel lines of roughness data, here only a single line is used corresponding to the centre of the contact. Sample results are shown in Fig. 2 for a wheel load of 50 kN, a wheel radius of 0.46 m, and rail transverse radius of curvature 0.46 m. The corresponding contact patch length is 5.31 mm. The dotted lines show the results for the six sets of wheel roughness and the thick solid line represents the average of these. Results are plotted against frequency for a train speed of 100 km/h.

In the figure, results are also shown from the 3D DPRS model. Results from the two models are similar for frequencies up to about 2.5 kHz (wavelengths down to about 11 mm). Above this frequency results for the 2D mattress model are a few dB higher.

Although differences of up to 5 dB occur, probably due to correlation effects across the contact width, the overall trends are well reproduced by this simple model. The average difference over all one-third octave bands is less than 2 dB.

3. Other models of the contact filter effect

3.1. Average deflection over the contact

The simplest form of averaging for the contact is to calculate the mean deflection over the nominal contact length, i.e. the mean roughness over this distance. The nominal contact length is the length in the absence of roughness. Note that in the actual situation the contact length may be more or less than nominal. This mean deflection is equivalent to convolving the input roughness with a rectangular window equal to the length of the contact. This provides an equivalent roughness, which can also be multiplied by the linearised stiffness to give the blocked force.

The filter effect of a rectangular window is well known (e.g. Ref. [9]), and for the quantities here is

$$G(\lambda) = \frac{\sin(2\pi a/\lambda)}{2\pi a/\lambda} = \frac{\sin(\pi f_{\mathrm{ND}})}{\pi f_{\mathrm{ND}}}, \tag{13}$$

where λ is the wavelength and a the semi-length of contact patch, and a dimensionless frequency has been defined as $f_{\mathrm{ND}} = 2a/\lambda$. The magnitude of Eq. (13) is shown in Fig. 3. Dips appear at $f_{\mathrm{ND}} = 1, 2, 3, \ldots$.

Because the mattress model is based on a set of linear springs, it too is basically a linear average and under many conditions should provide very similar results to the rectangular window. Some differences do occur because (i) in the window model a constant averaging length is used whereas in the mattress model the length varies with the contact conditions, and (ii) in the window model tensions are permitted within the contact, whereas in the mattress model contact is lost if tensions are predicted.

3.2. Analytical contact filter

For a circular contact patch of radius a, the filter transfer function derived by Remington [1] is

$$|H(k)|^2 = \frac{4}{\alpha}\frac{1}{(ka)^2}\int_0^{\tan^{-1}\alpha} J_1^2(ka\sec\psi)\,\mathrm{d}\psi, \tag{14}$$

where $k = 2\pi/\lambda$ is the roughness wavenumber, λ being the wavelength, and α is a parameter that describes the degree of correlation between roughness across the width of the contact zone at a given wavenumber. Large values of α imply poor correlation. It is unclear from Ref. [1] what value of α should be used. $|H(k)|$ is the filter weighting applied to the roughness amplitude at wavenumber k.

The result of this model, $|H(k)|$, is shown in Fig. 3 for a value of α of 0.1 (corresponding to high correlation across the contact width). It can be seen that the dips in the filter occur at values of f_{ND} that are greater than

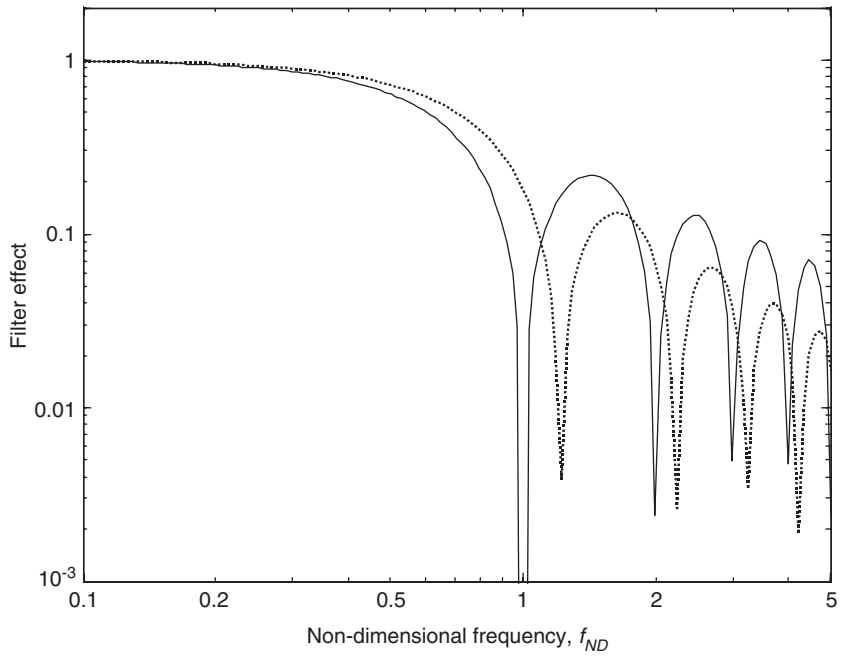

Fig. 3. Contact filter effect for rectangular window (—) and from Remington analytical model for $\alpha = 0.1$ ($\cdots\cdots$).

those from the rectangular window and that the filter has a greater attenuation at high frequencies than the rectangular window.

4. Boussinesq analysis

To provide reference data, a Boussinesq analysis was programmed in MATLAB® to generate "blocked force", i.e. the force assuming that distant points on the two contacting bodies maintain a constant separation when a roughness is interposed between them. As an alternative, deflection was also calculated for a known force, which was then suitable for implementation in a time-stepping dynamic model.

In the Boussinesq analysis the deflection is specified around a point load on a uniform half-space [2,7], as shown in Fig. 4(a). To extend this analysis to a pair of contacting bodies, the contact zone is divided into a regular grid of points. A series of loads is considered at the nodes of the grid, together with a corresponding set of displacements. If the load distribution at these points is known for the contact between the two bodies, using superposition the resultant displacement at any point can be found. Remington and Webb [2] show how this can be expressed in matrix terms as

$$\{\mathbf{u}\} = [\mathbf{A}]\{\mathbf{P}\}, \tag{15}$$

where $\mathbf{u}$ is a vector of displacements at each node, $\mathbf{P}$ is a vector of forces at each node and $\mathbf{A}$ is a matrix of deflections as in Fig. 4(a) described in Ref. [2].

In this case, the load at each point on the contacting bodies is not known. Instead the displacement is known, although only for points within the contact itself. Beyond the contact region the load is zero and the displacement is unknown. In this circumstance the problem becomes: given the displacements within the contact area, find the loads within the contact area and the displacements outside it.

To solve this problem, Eq. (15) is applied to points within the contact area alone. However, the extent of the contact is not known a priori, so an iterative process must be followed until the contact conditions are satisfied. Once the contact conditions are satisfied and the load distribution within the contact zone is determined, the loads outside the contact zone are set equal to zero, and Eq. (15) used with an extended $\mathbf{A}$ matrix to calculate the required distribution of displacements. In Fig. 4(b) is shown the prediction for a loaded sphere on a 2D cosinusoidal roughness.

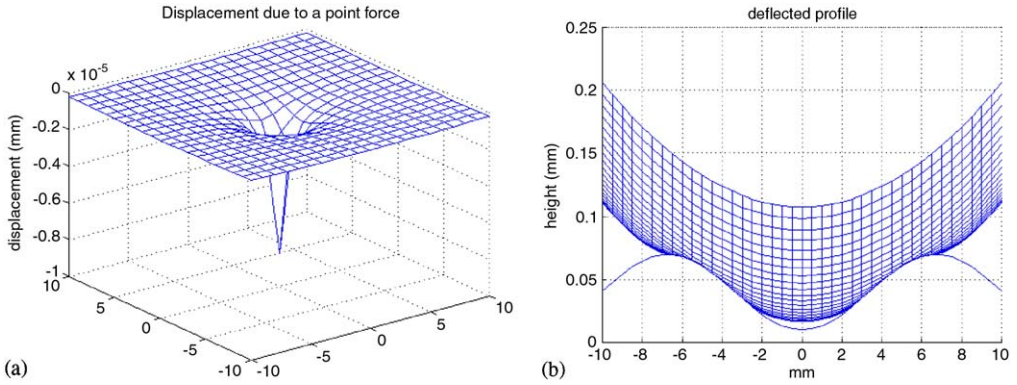

Fig. 4. Boussinesq predictions for: (a) displacement around a concentrated load on a half-space; (b) loaded sphere on a 2D cosinusoidal roughness.

For an analysis based on a constant load, an extra check is made on the total load, and the height of the wheel is adjusted before the next iteration. The linear contact stiffness is used to determine the extent of this adjustment. Once this has converged, the resulting contact deflection is used as a measure of the filtered roughness.

The precision of the Boussinesq analysis was investigated by comparing its predictions for the contact between a sphere and a smooth plane with the results of classical Hertzian analysis. For the mesh size used, the typical discrepancy in total load was an overestimate of about 1.5%.

5. Comparison of results

5.1. Cosinusoidal roughness

Fig. 5 shows the total load plotted against roughness amplitude for a nominal initial deflection of 40 μm (i.e. deflection in the absence of roughness). The upper results correspond to the load at a roughness peak and the lower results to that at a trough. The wavelength is $3a$, or 1.5 times the contact patch length.

Predictions using the mattress model and the rectangular window (average) are quite similar even at large amplitudes of the cosinusoid.

The results for the Boussinesq analysis differ noticeably from the rest, even at amplitudes in the middle of the selected range. The most significant difference is when the contact is at the trough. This can be expected from Fig. 4(b), because after a certain amplitude is reached, contact is lost in the trough, and the load is taken by the flanks of the two neighbouring peaks. In Fig. 5, for amplitudes greater than 25 μm the load at the trough is greater than on a smooth plane, because at this amplitude the curvature of the roughness is much tighter than the curvature of the wheel, and this effect is marked. The ratio of radius of curvature at the trough to the radius of curvature of the wheel is therefore significant, and this curvature ratio is used as a parameter in subsequent analysis.

In Fig. 6 the results of the Boussinesq analysis, 2D mattress model, rectangular window and the Remington analytical model [1] are compared for an amplitude based on a curvature ratio of 10, over a range of dimensionless frequencies ($f_{\mathrm{ND}} = 2a/\lambda$), and smoothed into one-third octave bands. The mattress model gives results that are within 3 dB of those of the more exact Boussinesq analysis. Even the simple rectangular window gives results that are within 4 dB of those of the Boussinesq analysis. The Remington analytical model, however, deviates from it by up to 10 dB in the frequency range considered.

5.2. Dipped rail

Joints in continuously welded rails that are made in the field can result in a cusp-like discontinuity, typically of the form represented in Fig. 7. This curve has been constructed from two intersecting quadratic

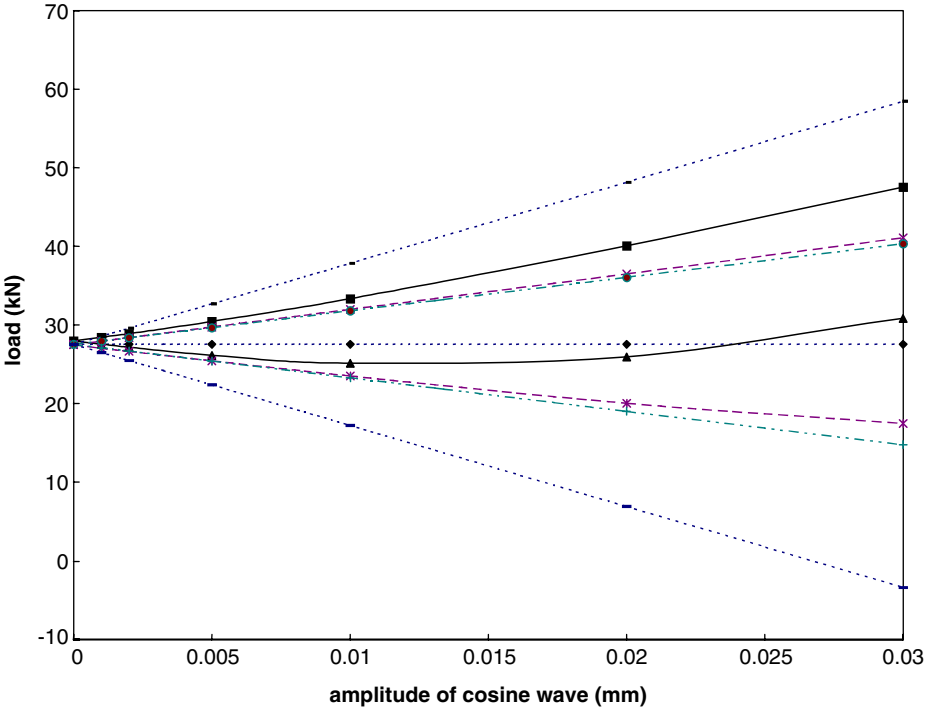

Fig. 5. Load versus amplitude of cosine wave, initial deflection 40 μm, wavelength 1.5 × contact length ($2a$). · · · ♦ · · · contact with plane; –■– Boussinesq peak; –▲– Boussinesq trough; - × - mattress peak; -*- mattress trough; - · · ● - rectangular window peak; - · · + - rectangular window trough; · · · - · · · no filter (linearised Hertzian spring).

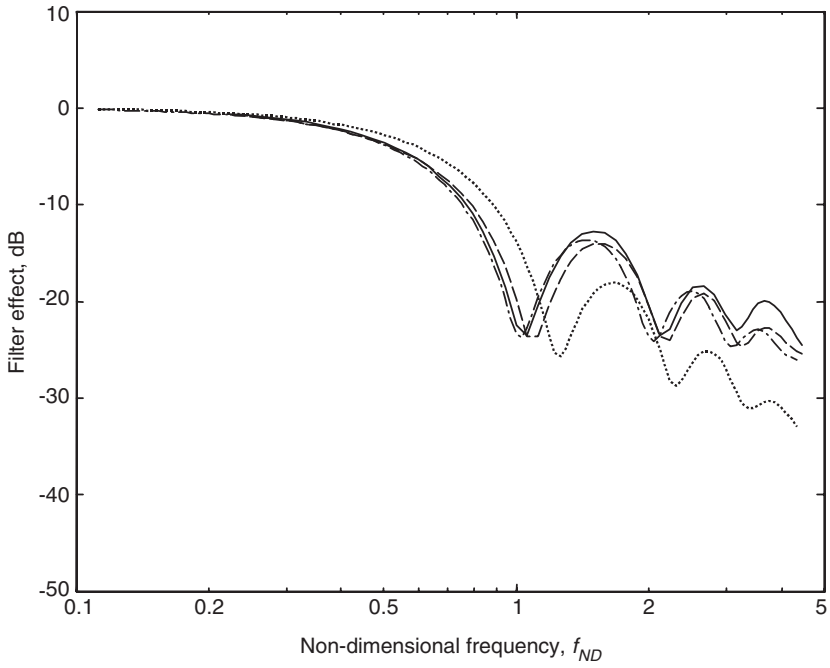

Fig. 6. Contact filter effect for constant curvature, curvature ratio 10 from various models, smoothed into one-third octave bands. — Boussinesq; – – – 2D mattress; – · – · rectangular window; · · · · · · Remington analytical model.

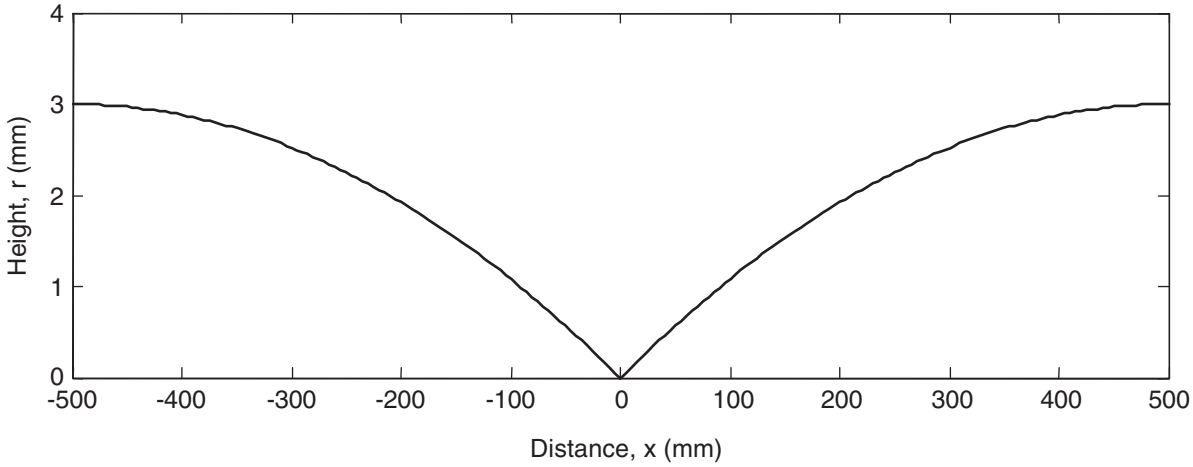

Fig. 7. Idealised representation of dipped rail shape, height 3 mm, overall length 1 m.

curves [6], each with a length of $l = 500$ mm and a depth at the intersection of $h = 3$ mm. The equation for this shape is

$$r(x) = 2h\left(\frac{|x|}{l}\right) - h\left(\frac{x}{l}\right)^2, \tag{16}$$

which is arranged to give $r(0) = 0$, $r(\pm l) = h$.

At first sight it appears that the adjusted radius (half-size) of the 2D mattress model would lead to gross differences when it encountered such a dipped rail, because it would go further towards the point of the cusp. Detailed geometrical considerations, however, have shown that this will not usually be as significant as at first might be supposed. Results here confirm this assessment.

Taking the whole 1 m long dipped profile of Fig. 7 and the corresponding filtered profiles obtained using the Boussinesq and mattress models, the Fourier transform of these profiles has been taken and converted into one-third octave bands. By forming the difference relative to the raw input an estimate is obtained of the filtering effect. The results are given in Fig. 8, plotted against the non-dimensional spatial frequency, f_{ND} used earlier, based as before on the nominal contact patch length of the wheel on a *flat* rail.

Compared with the results for sinusoidal roughness in Fig. 6, the filter effect here shows some differences. Firstly, the dips do not occur at a non-dimensional frequency of 1, 2, etc. but at rather higher frequencies. So, although the contact patch is *elongated*, the frequency of the dip corresponds to a wavelength that is *shorter* than the contact patch length for contact on a flat rail. Secondly, the attenuation at high frequencies is not as large as seen for sinusoidal roughness. Thirdly, the results from the mattress model differ from those of the Boussinesq analysis for non-dimensional spatial frequency between about 1 and 2. At higher frequency, however, the level of attenuation is similar for the two models.

Overall the differences between the Boussinesq and mattress models are not great, indicating that the mattress model could be used fairly reliably. However, the frequency domain filter effect determined from sinusoidal roughness (Fig. 6), shown here for comparison, cannot be used for the dipped rail profile. Unlike the case of sinusoidal roughness, the results have also been found to be load-dependent, even when plotted against non-dimensional spatial frequency.

5.3. Mattress model in a time-domain wheel/rail interaction model

The 2D mattress contact filter has been implemented in the time-domain wheel/rail interaction model of Refs. [4–6], incorporating it at each time step. The wheel was modelled by its unsprung mass, a 'modal' spring and a small mass at the contact of 3 kg, and the rail by the fourth-order state-space model of Refs. [4,5].

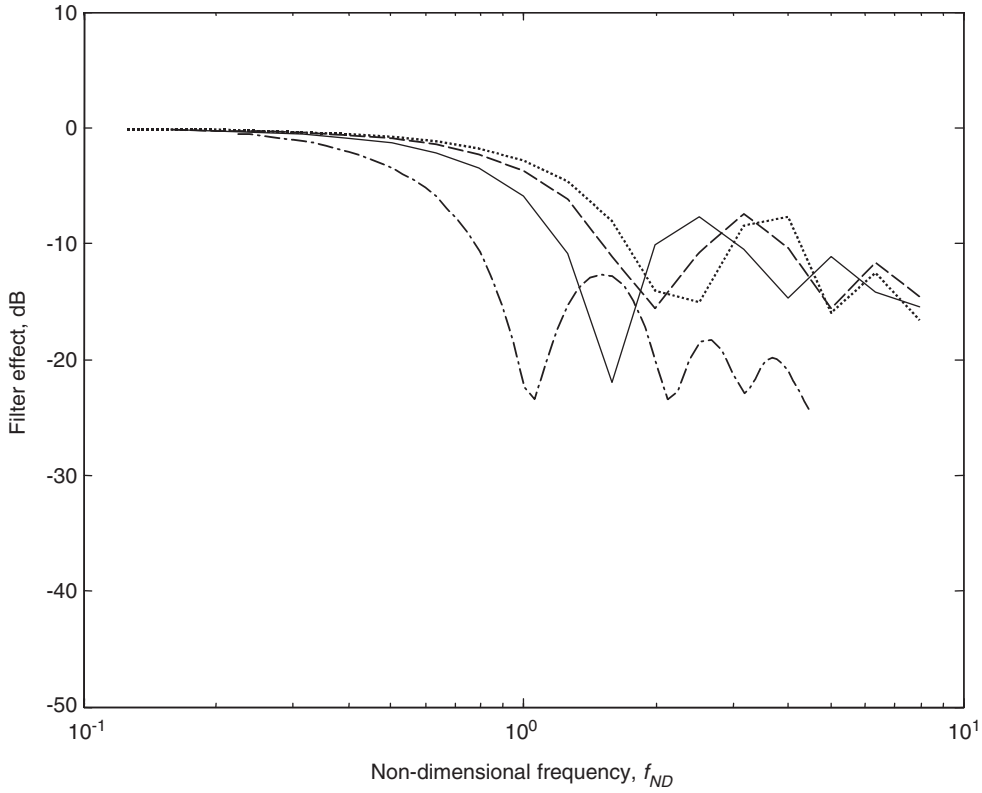

Fig. 8. Contact filter effect obtained on a dipped rail. — 50 kN mattress; – – – 50 kN Boussinesq; · · · · · · 30 kN Boussinesq; – · – · Boussinesq sinusoidal.

Results are shown in Fig. 9 for typical surface roughnesses corresponding to a block-braked wheel and a corrugated rail. The corrugated rail roughness was significantly higher in amplitude.

The dynamic model was run (a) with roughnesses that had been filtered using the 2D quasi-static mattress model (Section 2) but with no contact filter in the interaction model and (b) with the unfiltered roughnesses but including the contact filter in the interaction model. The contact filter effect is calculated by taking the difference between the results from these two runs and adding it to the contact filter effect obtained from the quasi-static contact filter (i.e. the difference in the inputs used). In Fig. 9, separate results are shown based on the contact force, rail vibration or the wheel vibration. The results from applying the quasi-static contact filter (Section 2) to these roughness profiles are also shown.

Similar trends are present in each case, but the result from the contact force differs from that obtained from the wheel or rail responses. Some of the discrepancies between the different dynamic results at high frequencies may be due to inadequacies in the time-stepping calculation. For the higher amplitude roughness (corrugated rail), the results deviate from those of the earlier quasi-static contact filter, and this is probably due to the presence of nonlinear effects in the wheel/rail interaction force at high amplitudes.

6. Conclusions

A 2D mattress model of elastic contact has been developed. It has been shown that it can be used to represent the contact filter effect between a wheel and a rail. However, it is necessary to adjust the wheel radius in order to ensure the correct contact patch length for a given wheel load and static deflection. Results agree with those from a 3D DPRS model with a maximum discrepancy of 5 dB and an average difference of less than 2 dB.

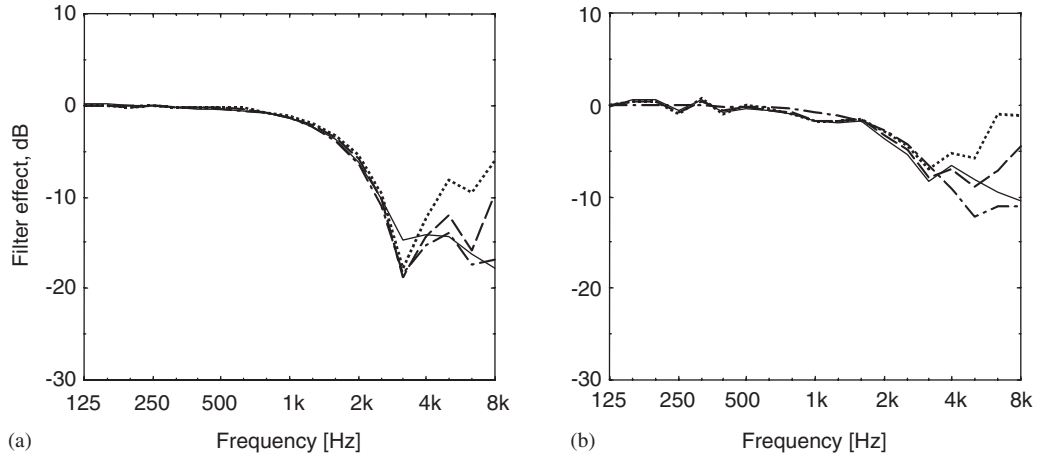

Fig. 9. Effect of introducing contact filter into dynamic model using roughness data: (a) for block-braked wheel roughness at 100 km/h, 25 kN load; (b) for corrugated rail roughness at 140 km/h, 25 kN load. — force; – – – rail vibration; · · · · · · wheel vibration; – · – · quasi-static filter.

Results of a Boussinesq model have been compared with a 2D mattress model and a simple rectangular window. Under the conditions evaluated, the mattress model is likely to give a good estimate of the behaviour predicted by the more complete Boussinesq model, with no significant bias; results in one-third octave bands are found to be within 3 dB of those from the Boussinesq model. A simple rectangular window gives a similar filtering effect to the mattress model for sinusoidal inputs. Under some conditions it may be convenient to use the rectangular window. However, this should not be used on isolated features such as a dipped rail.

Remington's analytical model has also been evaluated and found to give too large an attenuation at high frequencies. A similar conclusion was reached from a comparison with the DPRS model [3].

The filter effect on a dipped rail joint has also been investigated using both the Boussinesq model and the 2D mattress model. The two models agree well here too. However, it is noted that the filter effect is quite different from that obtained for sinusoidal roughness of moderate amplitude.

The 2D mattress model only requires a single roughness input profile and can be readily included into a time-stepping model of wheel/rail interaction. When this was done similar results were obtained to those from the quasi-static filtering of roughness if moderate roughness amplitudes were present. However, with large amplitudes where nonlinear effects are significant, including dipped rail joints, incorporating the dynamic model at each time step gives different results at high frequencies.

Acknowledgements

This work was partly carried out during the sabbatical leave of the first author from The University of New South Wales, and its context was the project "Nonlinear effects at the wheel rail interface and their influence on noise generation", grant GR/M82455, supported by the Engineering and Physical Sciences Research Council of the UK.

References

[1] P.J. Remington, Wheel/rail rolling noise, I: theoretical analysis, *Journal of the Acoustical Society of America* 81 (1987) 1805–1823.

[2] P.J. Remington, J. Webb, Estimation of wheel/rail interaction forces in the contact area due to roughness, *Journal of Sound and Vibration* 193 (1996) 83–102.

[3] D.J. Thompson, The influence of the contact zone on the excitation of wheel/rail noise, *Journal of Sound and Vibration* 267 (3) (2003) 523–535.

[4] T.X. Wu, D.J. Thompson, Theoretical investigation of wheel/rail non-linear interaction due to roughness excitation, *Vehicle System Dynamics* 34 (4) (2000) 261–282.
[5] T.X. Wu, D.J. Thompson, A hybrid model for the noise generation due to railway wheel flats, *Journal of Sound and Vibration* 251 (1) (2002) 115–139.
[6] T.X. Wu, D.J. Thompson, On the impact noise generation due to a wheel passing over rail joints, *Journal of Sound and Vibration* 267 (3) (2003) 485–496.
[7] K.L. Johnson, *Contact Mechanics*, Cambridge University Press, Cambridge, 1985.
[8] D.J. Thompson, Wheel/Rail Noise: Theoretical Modelling of the Generation of Vibrations, PhD Thesis, University of Southampton, 1990.
[9] R.B. Randall, *Frequency Analysis*, Brüel and Kjaer, Naerum, Denmark, 1987 ISBN 87 87355 07 8.